

NJC

Accepted Manuscript



This is an *Accepted Manuscript*, which has been through the Royal Society of Chemistry peer review process and has been accepted for publication.

Accepted Manuscripts are published online shortly after acceptance, before technical editing, formatting and proof reading. Using this free service, authors can make their results available to the community, in citable form, before we publish the edited article. We will replace this *Accepted Manuscript* with the edited and formatted *Advance Article* as soon as it is available.

You can find more information about *Accepted Manuscripts* in the [Information for Authors](#).

Please note that technical editing may introduce minor changes to the text and/or graphics, which may alter content. The journal's standard [Terms & Conditions](#) and the [Ethical guidelines](#) still apply. In no event shall the Royal Society of Chemistry be held responsible for any errors or omissions in this *Accepted Manuscript* or any consequences arising from the use of any information it contains.

Cite this: DOI: 10.1039/c0xx00000x

www.rsc.org/xxxxxx

ARTICLE TYPE

Cyano-bridged copper(II)-copper(I) mixed-valence coordination polymer as source for copper oxide nanoparticles with catalytic activity in C-N, C-O and C-S cross-coupling reactions

Manoj Trivedi^{a*}, Sanjeev kumar Ujjain^a, Raj Kishore Sharma^a, Gurmeet Singh^a, Abhinav Kumar^b, and Nigam P. Rath^{c*}

Received (in XXX, XXX) Xth XXXXXXXXXX 20XX, Accepted Xth XXXXXXXXXX 20XX

DOI: 10.1039/b000000x

Cyano-bridged copper(II)-copper(I), mixed valence polymer, namely $\{[\text{Cu}_4(\text{CN})_5(\text{C}_5\text{H}_5\text{N})_4]\}_n$ (**1**), was synthesized and characterized by elemental analysis, IR, thermogravimetric analysis, differential scanning calorimetric analysis, and single crystal X-ray crystallography. Single crystal X-ray studies show that the coordination polymer **1** is linked by the cyanide anions with μ - $1\kappa\text{N}:2\kappa\text{C}$ bridging modes to the copper centers and generate the two-dimensional (2D) layered network. The coordination polymer **1**, on pyrolyzing, yielded copper oxide nanoparticles, which have been characterized by TEM and powder X-ray diffraction. The catalytic properties of the resulting copper oxide nanoparticles have also been studied for C-N, C-O, and C-S cross-coupling reactions with aryl halides. The C-N, C-O and C-S coupling products were obtained in moderate to good yields (66-90%, 72-98%, 50-86%), respectively.

Introduction

During the last few years considerable research efforts have been made on the design of metal coordination polymers for their intriguing architectures and potential applications in many fields, such as catalysis, magnetic devices, separation, molecular recognition, non-linear optics, hydrogen storage, etc.¹ Among these metal coordination polymers, copper cyanide systems have received special interests due to their fascinating structural frameworks, superior physical and chemical properties, and potential applications in many fields.² The cyanide group is a versatile ligand that can act as a mono-dentate as well as a μ_2 -, μ_3 -, or μ_4 -bridging multi-dentate ligand, while copper possesses versatile coordination properties and can adopt two-, three-, four-, five-, or six-coordination to form diverse geometries. The strong bridging tendency of the cyanide group often assists the attainment of suitable architectures for extended luminescent interactions. Therefore, the self-assembly of copper cyanide can generate long-lived and highly efficient luminescent materials with variable structures, which sometimes exhibit intriguing topological architectures.³ Recently, a large number of cyanide-bridged complexes with intriguing topologies and fascinating properties have been reported, such as $\text{ZnM}(\text{CN})_4$ ($\text{M} = \text{Ni}, \text{Pd}, \text{Pt}$)⁴, $\{[\text{Mn}(\text{bpy})(\text{H}_2\text{O})_2\text{Fe}(\text{CN})_5(1\text{-CH}_3\text{im})]\cdot\text{H}_2\text{O}\}_n$ ⁵, $\text{Zn}(\text{CN})_2$ ⁶, $\text{Ln}_2\text{Cu}_5(\text{ina})_6(\text{CN})_{5.5}\cdot 4\text{H}_2\text{O}$ ($\text{Ln} = \text{Nd}, \text{Eu}, \text{Tb}, \text{Gd}, \text{Sm}$)⁷, $\text{Zn}[\text{Au}(\text{CN})_2]_2$ ⁸, $\text{Ag}_3\text{Co}(\text{CN})_6$ ⁹, $[\text{Ag}(\text{CN})_2\text{Mn}(\text{L}^1)][\text{Ag}(\text{CN})_2]^{10}$, $[\text{Cu}_2\text{Ni}(\text{dien})(\text{I-CN})_5]_n$ ¹¹, $\text{Ag}(\text{CN})_2\text{Mn}(\text{L}^2)[\text{Ag}(\text{CN})_2]\cdot 1.5\text{H}_2\text{O}$ ¹⁰, and $[\text{Au}(\text{CN})_2\text{Mn}(\text{L}^2)][\text{Au}(\text{CN})_2]\cdot 1.5\text{H}_2\text{O}$ ¹⁰. When an auxiliary

N-donor ligands are introduced into $[\text{CuCN}]$ framework, they lead to the formation of a variety of coordination networks.¹² Thus, the prospect of $[\text{CuCN}]$ -based coordination polymers through a systematic change of auxiliary N-donor ligands provides an impetus for further research on polymer architectures. Although great attention has been focused to the coordination polymers particularly copper having nanostructures with specific morphology have rarely been reported.¹³ Recently, CuO has engendered wide attention because of their versatile properties and potential applications. For example, CuO has been widely used in heterogeneous catalysts, gas sensors, superconductor industry, optical switching devices, solar cells and lithium ion batteries.^{14,15} Nanostructural CuO might exhibit special physical and chemical properties that are different from the bulk materials. Moreover, the size and morphology of CuO will cause a great impact on the properties and potential applications of materials. With these aspects in mind and in the quest for some beautiful and fascinating networks herein, we report the synthesis and structural characterization of cyano-bridged mixed-valence copper coordination polymer $\{[\text{Cu}_4(\text{CN})_5(\text{C}_5\text{H}_5\text{N})_4]\}_n$ (**1**) and the CuO nanoparticles obtained by their thermal treatment. We also discuss the catalytic properties of the CuO nanoparticles in cross-coupling reactions of amides, imidazoles, amines, phenol and benzenethiol with aryl halides.

Experimental

Materials and Methods

All the synthetic manipulations were performed under aerobic condition. The solvents were dried and distilled before use following the standard procedures.¹⁶ Copper cyanide, ammonia solution, pyridine, and CuO powder (all Aldrich) were used as received. Elemental analysis was performed on a Carlo Erba Model EA-1108 elemental analyzer and data of C, H and N is within $\pm 0.4\%$ of calculated values. IR(KBr) was recorded using Perkin-Elmer FT-IR spectrophotometer. Electronic and emission spectra for **1** were obtained on a Perkin Elmer Lambda-35 and Horiba Jobin Yvon Fluorolog 3 spectrofluorometer, respectively. The structural characterization of the fired products at 500°C were done using X-ray diffraction (XRD) measurements using Bruker D8 Discover X-ray diffractometer, with Cu K α_1 radiation ($\lambda = 1.5405 \text{ \AA}$). For TEM measurements small quantity of the pyrolyzed product was dispersed in isopropyl alcohol by sonicating for about 30 min. 5 ml of the suspension was put on copper grids using a microliter pipette. The TEM measurements were carried out using a FEI TECNAI G2200 kV transmission electron microscope. Rietveld analysis of all samples was performed using the Fullprof program.

Preparations

$\{[\text{Cu}_4(\text{CN})_5(\text{C}_5\text{H}_5\text{N})_4]\}_n$ (**1**)

Copper cyanide (0.178 g, 2 mmol) was added slowly to a solution of CH₃OH (10 mL), and CH₂Cl₂ (10 mL) containing liquid NH₃ (0.1 mL, 6 mmol). The resulting solution was stirred at room temperature for 6 hours. Slowly, color of the solution changes from creamy to blue color. The resulting solution was filtered and layered with pyridine. Dark blue color block shaped crystals suitable for X-ray studies were obtained after four weeks. Yield: (0.980 g, 70%). Anal. Calc. for C₂₅H₂₀N₉Cu₄: C, 42.82; H, 2.85; N, 17.98. Found: C, 42.93; H, 2.95; N, 18.10. IR(cm⁻¹, nujol): $\nu = 3588, 3350, 3268, 2922, 2854, 2723, 2247, 2137, 2105, 1609, 1462, 1377, 1265, 1243, 1211, 721, 682$. UV/Vis: λ_{max} ($\epsilon/\text{dm}^3 \text{ mol}^{-1} \text{ cm}^{-1}$) = 273(17538). TGA Calcd for (Py)₃: 33.8. Found: 31.6 (102-314°C). Calcd for (CN)₃: 11.1. Found: 11.2 (314-606°C).

X-Ray data collection and structure determination

Crystals suitable for single crystal X-ray analysis for $\{[\text{Cu}_4(\text{CN})_5(\text{C}_5\text{H}_5\text{N})_4]\}_n$ (**1**), were grown from slow diffusion at room temperature. Preliminary data on the space group and unit cell dimensions as well as intensity data were collected on X-calibur S oxford diffractometer using graphite monochromatized Mo-K α radiation. CrysAlisPro, Agilent Technologies software packages¹⁷ were used for data collection and data integration for **1**. Structure solution and refinement were carried out using the SHELXTL-PLUS software package.¹⁸ The non-hydrogen atoms were refined with anisotropy thermal parameters. All the hydrogen atoms were treated using appropriate riding models. The computer programme PLATON was used for analyzing the interaction and stacking distances.¹⁸ The refinement details for **1** is summarized in Table 1.

General Procedure for C-N Cross-Coupling Reactions

Nitrogen nucleophile (1.2 mmol), aryl iodide (1 mmol), CuO nanoparticles (5 mol %), and KOH (1.5 mmol) were stirred at 110°C in a 1:3 mixture of DMSO/*t*-BuOH (1 mL). The progress of the reaction was monitored by TLC using EtOAc and hexane

as eluent. After completion, the reaction mixture was treated with EtOAc (10 mL) and water (3 mL). The organic layer was separated, and the aqueous layer was extracted with EtOAc (3 \times 5 mL). The combined organic solution was washed with brine (3 \times 5 mL) and water (1 \times 5 mL). Drying (anhydrous Na₂SO₄) and evaporation of the solvent yielded a residue, which was purified on short pad of silica gel using EtOAc and hexane as eluent.

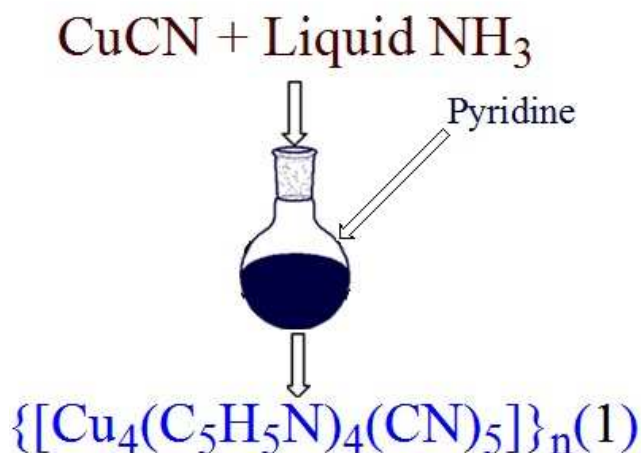
General Procedure for C-O and C-S Cross-Coupling Reactions

Oxygen or sulfur nucleophile (1 mmol), aryl iodide (1.2 mmol), CuO nanoparticles (2.5 mol %), and KOH (1.5 mmol) were stirred at 80-110°C in DMSO (1 mL) under N₂ atmosphere. Monitoring of the reaction, workup procedure, and purification of the C-O and C-S cross-coupled products were performed as described for the C-N cross-coupling reactions.

Results and discussion

Synthesis

The new cyano-bridged coordination polymer $\{[\text{Cu}_4(\text{CN})_5(\text{C}_5\text{H}_5\text{N})_4]\}_n$ (**1**), was obtained in significant yield by the reaction of the CuCN with liquid NH₃ in 1:3 stoichiometric ratio in a mixture of dichloromethane and methanol (1:1v/v) under stirring conditions at RT and then layered with pyridine (Scheme 1). Complex **1** is air stable solid, insoluble in water and other common organic solvents but soluble in dimethyl sulfoxide and do not show any signs of decomposition in solution upon exposure to air for days. The elemental analysis was consistent with their chemical formula.



Scheme 1. Synthetic routes for the coordination polymer **1**.

Spectroscopy

The IR spectrum of the complex **1** showed a strong peak at 2137 cm⁻¹, and 2105 cm⁻¹, which may be assigned to the bridging cyanide groups and higher than that of terminal cyanide ion (approx. 2050 cm⁻¹) (See S1, supporting material). Concerning the two peaks in the IR spectrum, it probably arises from the contribution of Cu^I and Cu^{II} bridging modes.

Description of Crystal Structure

One X-ray structure emerged in the current study. A refinement detail for **1** is summarized in Table 1, and selected bond lengths and angles are presented in Tables 2. Complex **1** crystallizes in the monoclinic space group $C2/c$. The X-ray structure of **1** is depicted in Fig. 1. Complex **1** has an infinite two-dimensional architecture with three crystallographically independent Cu atoms bridged by cyanide groups in the symmetric unit. There are three kinds of coordination modes for the Cu atoms: the first monovalent Cu atom (Cu1) is coordinated by two (μ_2, η^2) -cyanide [N(1)-C(1)= 1.145(3) Å, C(3)-N(3) = 1.137(3) Å] atoms, one κ^1 -pyridyl rings [Cu(1)-N(5) = 2.101(2) Å] and one copper metal Cu(1)-Cu(1)^{#1} = 2.625(5) exhibits a distorted

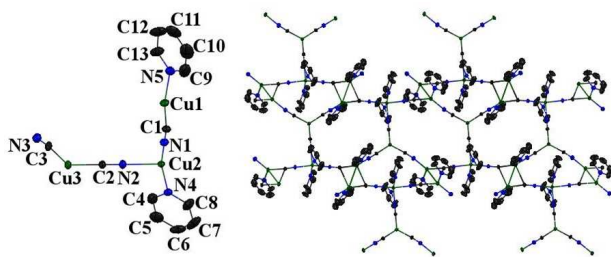


Fig. 1 The asymmetrical unit of **1** is on the left. The right diagram shows the 2D polymeric framework of **1**. tetrahedral coordination environment, whereas the second divalent Cu atom (Cu2) is coordinated by three (μ_2, η^2) -cyanide [N(1)-C(1)= 1.145(3) Å, C(3)-N(3) = 1.137(3) Å] atoms, and two κ^1 -pyridyl rings [Cu(2)-N(4)= 2.0328(18)Å] and exhibits distorted square bipyramidal coordination environment. The remaining third Cu atom (Cu3) display distorted trigonal planar geometry consisting of three cyanides in (μ_2, η^2) -manner [N(2)-C(2)= 1.134(4) Å, C(3)-N(3)= 1.137(3) Å]. All Cu-N and Cu-C bond distances are in the range of 1.929(2) to 2.143(3) Å and 1.921(2) to 2.475(2) Å, respectively and comparable to the values reported in literature.¹² The alternating linkages of the six Cu atoms and six cyanide groups form an 18-membered hexagonal repeating unit [Cu₆(CN)₆] in the lattice (Fig. 2). The approximate size of 18-membered hexagonal rings is 9.425 x 11.875 Å² based on the metal-metal distances, respectively.

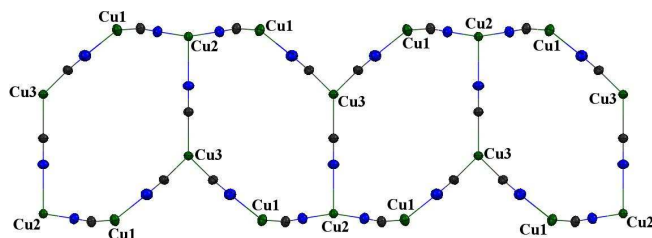


Fig. 2 Layered structure of the **1** showing the 18-membered hexagonal rings viewed along the c -axis.

The copper atoms are bridged by the cyanide ligands to afford a two dimensional (2-D) layered network (Fig. 3a). Within the framework of **1**, hexagonal channels are present (Fig. 3b). PLATON analysis shows that the number of void grid points is 0 and percentage filled space are 62.9%. Unit cell contains no residual solvent accessible void.

In DMSO solution, complex **1** exhibited an intense absorption band in the range of 273 nm (See S2, supporting material), which

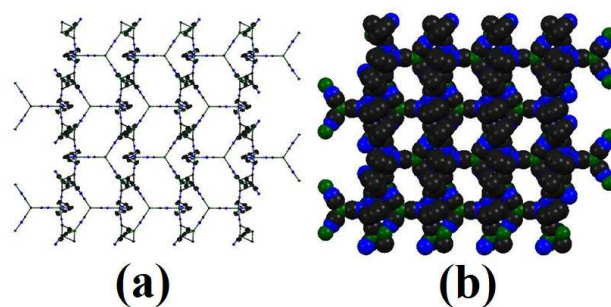


Fig. 3 (a) 2-D layered network of **1**, and (b) Spacefill model of **1** showing the channels in the 2D framework.

Table 1. Crystallographic data for **1**.

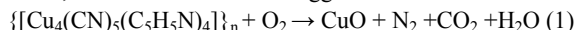
Empirical Formula	C ₂₅ H ₂₀ N ₉ Cu ₄
FW	700.66
crystal system	Monoclinic
space group	$C2/c$
a, Å	20.3823(13)
b, Å	10.5171(4)
c, Å	15.1002(9)
α , deg	90.00
β , deg	120.961(8)
γ , deg	90.00
V, Å ³	2775.7(3)
Z	4
d_{calc} , g cm ⁻³	1.677
μ , mm ⁻¹	3.055
T, K	293 (2)
R _i all	0.0419
R _i [I > 2 σ (I)]	0.0333
wR ₂	0.0839
wR ₂ [I > 2 σ (I)]	0.0796
GoF	1.064

can be ascribed to a metal-to-ligand charge-transfer transition at room temperature. Complex **1** is found to be luminescent at room temperature in DMSO solution. Complex **1** showed strong luminescence behaviour, having an excitation peak 273 nm, produces two broad emission peak centered at 360 nm and 651nm, respectively (See S3, supporting material). We have also performed solid-state luminescence of complex **1** (See S4, supporting material), which indicated that complex **1** is stable in solution and no decomposition of the framework occurs. Luminescence response for this complex is red-shifted and due to metal-to-ligand charge-transfer (Cu \rightarrow CN, MLCT), similar to those of other cyano metal complexes.¹⁹

Thermal and Differential scanning calorimetry

Thermogravimetric analysis (TGA) and Differential scanning calorimetry (DSC) were carried out on complex **1**. Mass losses, temperature ranges, and interpretations are presented in the experimental section. The representative TGA and DSC curve for complex **1** is shown in Fig. 4. The TGA traces revealed smooth loss of cyanide and pyridine, occurring in multiple stages, but always leaving copper oxide. This process began at temperatures as low as 100°C and as high as 450°C, but typically commenced around 100-878°C. The thermogram indicates that the pyridyl and cyano groups are removed sequentially, probably with the first being removed easily and the remainder more slowly as this decomposition correlates with a wide temperature range for the

loss of these groups in the TGA. Based upon TGA mass percent values, transformation of **1** is suggested:



The increase in weight from 550 to 750°C is observed from the thermogravimetric curves of the complex **1** due to the presence of residual copper which was finally oxidized to CuO under an air atmosphere. The DSC curve for complex **1** is characterized by two exothermic peaks located at 201°C and 606°C, attributed to the loss of pyridyl and cyanide ligands from the complex and its subsequent vaporization, respectively.

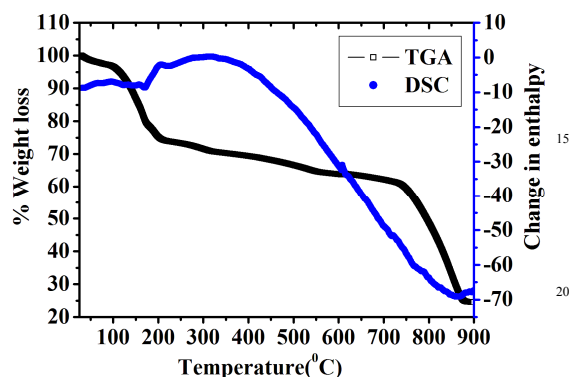


Fig. 4 TGA and DSC profiles of $\{[\text{Cu}_4(\text{CN})_5(\text{C}_5\text{H}_5\text{N})_4]\}_n$ (**1**) recorded under an air flow.

Table 2. Selected bond lengths (Å), and Bond angles (°) for **1**.

Cu(1)-C(1)	1.921(2)
Cu(1)-N(3)	1.929(2)
Cu(1)-N(5)	2.101(2)
Cu(1)-C(1) ^{#1}	2.475(2)
Cu(1)-Cu(1) ^{#1}	2.6525(5)
Cu(2)-N(1) ^{#2}	1.9790(17)
Cu(2)-N(1)	1.9790(17)
Cu(2)-N(4) ^{#2}	2.0328(18)
Cu(2)-N(4)	2.0328(18)
Cu(2)-C(2)	1.909(3)
Cu(2)-N(2)	2.143(3)
Cu(3)-C(3)	1.9386(19)
Cu(3)-C(2)	1.909(3)
N(1)-C(1)	1.145(3)
N(2)-C(2)	1.134(4)
N(3)-C(3) ^{#3}	1.137(3)
N(4)-C(8)	1.322(3)
N(4)-C(4)	1.327(3)
N(5)-C(13)	1.307(4)
N(5)-C(9)	1.319(4)
N(4)-Cu(2)-N(2)	100.93(5)
C(1)-Cu(1)-N(5)	106.50(9)
C(1)-Cu(1)-N(3)	136.17(9)
N(3)-Cu(1)-N(5)	106.03(9)
C(1)-Cu(1)-C(1) ^{#1}	107.00(7)
N(4)-Cu(2)-N(1)	89.38(7)
N(4) ^{#2} -Cu(2)-N(4)	158.14(11)
C(2)-Cu(3)-C(3)	122.76(6)
C(3)-Cu(3)-C(3)	114.47(12)
C(1)-N(1)-Cu(2)	177.50(18)
C(2)-N(2)-Cu(2)	180.0
C(3)-N(3)-Cu(1)	170.9(2)
N(1)-C(1)-Cu(1)	167.45(19)
N(3)-C(3)-Cu(3)	170.8(2)
N(2)-C(2)-Cu(3)	180.0

Solid state pyrolysis and Surface morphology

In order to study the nature and morphology of the product, the techniques such as X-ray diffraction (XRD), and transmission

electron microscopy (TEM) were employed and Rietveld refinement was used to analyze phase composition and structural parameters. We have performed pyrolysis experiments in air at 500°C for 10h. On pyrolyzing, complex **1**, was converted to pure copper oxide. Fig. 5 displays the observed (blue) and fitted (red) diffraction patterns with their differences (gray).

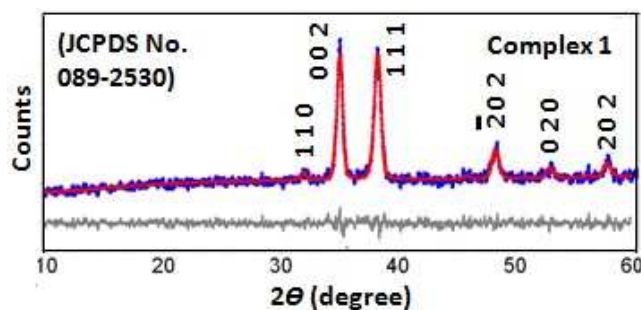


Fig. 5. Rietveld fitted powder XRD patterns CuO sample obtained from the complex **1**, fired at 500°C for 10 h.

Structural refinement of the XRD data reveals that the CuO sample is crystallized in the nearly single phase Base-centered monoclinic crystal structure (space group *C2/c*). The crystallographic parameters obtained from the refinements are listed in table 3.

Table 3. Rietveld refined parameters and Base-centred monoclinic distortion of CuO sample.

Samples	Complex 1
Space Group	<i>C2/c</i>
<i>a</i> [Å]	4.7267277
<i>b</i> [Å]	3.4680945
<i>c</i> [Å]	5.1769531
<i>V</i> [Å ³]	83.69595
<i>R</i> _{exp} (%)	9.20
<i>R</i> _p (%)	4.85
<i>R</i> _{wp} (%)	6.15

The positions of the peaks are in good agreement with literature values. Fig. 6 shows the TEM images, SAED patterns and histogram illustrating the morphology, lattice planes and size distribution of the CuO NPs obtained from complex **1**. Fig. 6a, shows the flower like morphology of CuO (50-70 nm) derived from complex **1**. This size is in close approximation to the crystallite size of 71 nm derived from Scherrers' equation. These flowers are composed of connected petals of particle size varies from 6 to 16 nm and the peak centred at about 10 nm as shown in the histogram (inset Fig. 6b). SAED pattern indicates the crystalline character exhibiting presence of (020), (111) and (110) planes for the CuO nanocrystals (Fig. 6b).

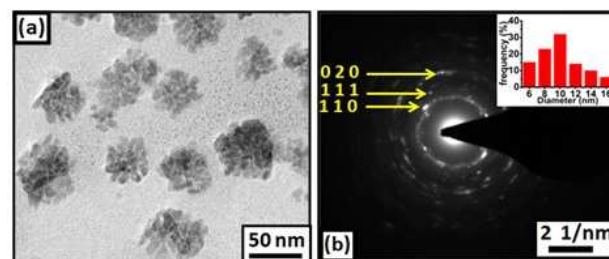
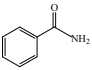
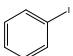
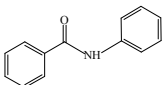
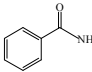
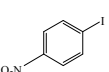
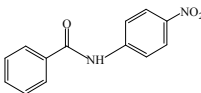
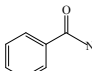
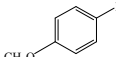
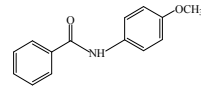
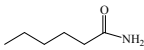
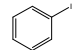
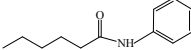
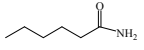
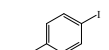
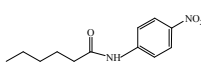
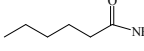
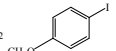
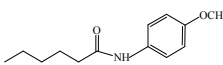


Fig. 6. TEM images of flower like CuO nanocrystals derived from complex **1** (a), SAED pattern showing different planes (b) and inset shows statistical representation for size distribution of flower like nanoparticles in the sample.

Catalytic application of the copper oxide nanoparticles

The copper oxide nanoparticles were examined as catalysts in the cross-coupling reactions of benzamide, hexanoamide, aniline, imidazole, phenol, and benzenethiol with various aryl halides in accordance with the previously reported methods by Punniyamurthy et al.²⁰. The C-N cross-coupling reactions were carried out in air, while the C-S and C-O cross-couplings gave the best results in nitrogen atmosphere. In our current observation, we have found that the resulting CuO nanoparticles showed lower catalytic activity than commercial CuO nanoparticles for these reactions. We have found nearly the similar activities as previously reported by Punniyamurthy et al.^{23a} that iodobenzene exhibited greater reactivity as compared to aryl bromides and aryl chlorides. Under these conditions, bromohalides and chlorohalides gave a low yield (<5%). In our studies, we have not isolated any homocoupled biaryl product. We have also found that no reaction occurred in the absence of copper oxide nanoparticles.

Table 4. CuO Nanoparticles Catalyzed Amidation of Aryl iodides.^a

S.No.	Amide	Aryl halide	Time (h)	Product	Yield (%)
1.			24		70
2.			24		60
3.			24		45
4.			24		90
5.			24		60
6.			24		50

^aCuO nanoparticles (5 mol %), amide (1.2 mmol), aryl iodide (1 mmol), and KOH (1.5 mmol) were stirred at 110°C in a 1:3 mixture of DMSO/*t*-BuOH (1 mL) for 24h.

Reactions of Amides, and Imidazoles

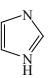
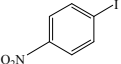
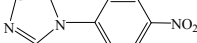
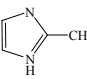
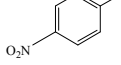
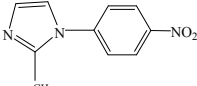
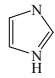
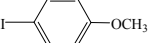
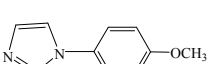
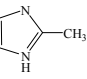
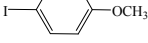
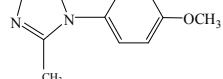
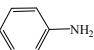
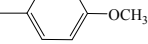
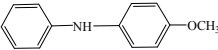
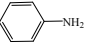
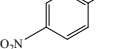
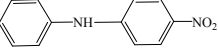
Benamide, and hexanoamide were tested as starting materials for C-N cross-coupling reactions with aryl iodides (Table 4). The yield of the cross-coupled products was 45-90%. During the course of experiment, it has been observed that 4-nitro-1-iodobenzene showed greater reactivity compared to 4-methoxy-1-iodobenzene. These reactions have been carried out in KOH as a

base to obtain moderate to good yield. As a consequence of these results, we further examined the reactions of substituted aryl iodides with imidazoles (Table 5). We have found that imidazole, 2-methylimidazole, and aniline underwent efficiently to give cross-coupled products up to 66-90% yield.

Reactions of Phenols

Phenol was tested as starting material for C-O cross-coupling reactions with various aryl iodides. We first checked the reaction of the phenol with iodobenzene. It was observed that iodobenzene efficiently coupled to give the C-O cross-coupled products in 72-98% yield (Table 6). The scope of this system was further examined with bromobenzene or chlorobenzene by varying the catalyst concentration (2.5 mol% to 5 mol%) and the temperature (110-130°C). We have found that low yield (<5%) of the cross-coupled products were obtained. We also examined the influence of aryl iodides having 3-NO₂, 4-NO₂, 4-Me, 2-OMe, 4-OMe substituents with phenol. We found that the reactions proceed to give the C-O cross-coupled products in 72-98% yield.

Table 5. CuO Nanoparticles Catalyzed reaction of imidazole and aniline with Aryl iodides.^b

S.No.	Substrate	Aryl iodide	Time (h)	Product	Yield (%)
1.			24		90
2.			24		85
3.			24		66
4.			24		88
5.			24		80
6.			24		90

^bCuO nanoparticles (5 mol %), substrate (1.2 mmol), aryl iodide (1 mmol), and KOH (1.5 mmol) were stirred at 110°C in a 1:3 mixture of DMSO/*t*-BuOH (1 mL) for 24h.

Reactions of Benzenethiol

Benzenethiol was tested as starting material for C-S cross-coupling reactions of various aryl iodides (Table 7). We have examined the reaction of benzenethiol with aryl iodides having 4-NO₂, 4-Br, 4-Me, and 4-OMe substituents. Benzenethiol efficiently coupled with aryl iodides having 4-NO₂, 4-Br, 4-Me, and 4-OMe substituents to give 50-86% yield of the C-S cross-coupled products.

Mechanism

The greater reactivity of the aryl iodide having an electron-withdrawing group compared to aryl iodide having an electron-

donating group indicates that the reactions proceed *via* oxidative addition followed by a reductive elimination process. These reactions are heterogeneous, and no leaching of the metal species was observed during the course of our reactions. As described in Fig. 7, the catalysis may be occurring on the surface of the CuO nanoparticles. The DMSO-stabilized CuO nanoparticles may react with aryl halide to give an intermediate (i). Then the excess positive charge developed on an intermediate (i) should be shared by surface of the CuO nanoparticles cluster (ii) and finally it may react with nucleophile to give an intermediate (iii) that can complete the catalytic cycle by reductive elimination of the desired cross-coupled product.

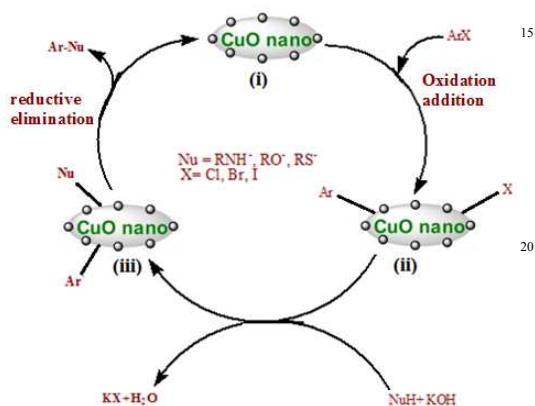


Fig. 7. Proposed reaction mechanism for CuO-nanoparticle-catalyzed cross-coupling reactions.

Table 6. CuO Nanoparticles Catalyzed Cross Coupling of phenol with Aryl iodides.^c

$\text{Phenol} + \text{Y-C}_6\text{H}_4\text{-I} \xrightarrow[\text{N}_2]{\text{CuO nanoparticles (1.5 equiv KOH), DMSO, 110}^\circ\text{C}}$ $\text{Phenol-O-C}_6\text{H}_4\text{-Y}$ Y = NO ₂ , CH ₃ , OCH ₃				
S.No.	Aryl iodide	Time (h)	Product	Yield (%)
1.		24		90
2.		24		98
3.		24		88
4.		24		72
5.		24		88

^cCuO nanoparticles (2.5 mol %), phenol (1 mmol), aryl iodide (1.2 mmol), and KOH (1.5 mmol) were stirred at 110°C in DMSO (1 mL) under N₂ atmosphere for 24h.

Table 7. CuO Nanoparticles Catalyzed C-S Cross-Coupling of benzenethiol with Aryl iodides.^d

$\text{Ph-SH} + \text{Y-C}_6\text{H}_4\text{-I} \xrightarrow[\text{N}_2]{\text{CuO nanoparticles (1.5 equiv KOH), DMSO, 80}^\circ\text{C}}$ $\text{Ph-S-C}_6\text{H}_4\text{-Y}$ Y = NO ₂ , CH ₃ , Br, OCH ₃					
S.No.	Substrate	Aryl iodide	Time (h)	Product	Yield (%)
1.			24		86
2.			24		60
3.			24		66
4.			24		50

^dCuO nanoparticles (2.5 mol %), thiophenol (1 mmol), aryl iodide (1.2 mmol), and KOH (1.5 mmol) were stirred at 80 °C in DMSO (1 mL) under N₂ atmosphere for 24h.

Conclusions

In this paper, we have reported a 2-D layered coordination network in which Cu(II) and Cu(I) centers are linked *via* CN bridges. On pyrolyzing, this complex gave copper oxide nanoparticles. In addition, TGA/DSC analysis, and PXRD data evidenced the occurrence of a clean vaporization process without premature side decompositions, and of a clear PXRD pattern dominated by the loss of the cyanide and pyridyl groups. We have also described a simple, and general procedure for the cross-coupling of nitrogen, oxygen, and sulfur nucleophiles with aryl iodides catalyzed by CuO nanoparticles in moderate to good yields. The work towards development of mixed valance coordination polymers containing various nitrogen donor ligands and their catalytic properties is in progress in our laboratory.

Acknowledgements

We gratefully acknowledge financial support by the Department of Science and Technology, New Delhi (Grant No. SR/FT/CS-104/2011). We also thank to the Director, USIC, University of Delhi, Delhi, for providing analytical, spectral and Single Crystal X-ray Diffraction facilities. We are thankful to Prof. W.S. Sheldrick and Dr. Heike Mayer-Figge for their help in crystallography and improvement of the paper. Special thanks are due to Professor P.J. Sadler, University of Warwick, UK, Professor Qiang Xu, National Institute of Advanced Industrial Science and Technology (AIST), Osaka, Japan for their kind encouragement. The authors sincerely thank the reviewers for their valuable suggestions and comments.

Notes and references

- ^aDepartment of Chemistry, University of Delhi, Delhi-110007, INDIA. Email: manojtri@gmail.com
- ^bDepartment of Chemistry, University of Lucknow, Lucknow-226007, INDIA

^cDepartment of Chemistry & Biochemistry and Centre for Nanoscience, University of Missouri-St. Louis, One University Boulevard, St. Louis, MO 63121-4499, USA. Email: rathn@umsl.edu

† Electronic Supplementary Information (ESI) available: CCDC reference numbers 868396 (1). For ESI and crystallographic data in CIF or other electronic format see DOI: 10.1039/b000000x/

- 1 (a) S. Horike, M. Dinca, K. Tamaki, J. R. Long, *J. Am. Chem. Soc.*, 2008, **130**, 5854; (b) F. M. Tabellion, S. R. Seidel, A. M. Arif, P. J. Stang, *Angew. Chem., Int. Ed.*, 2001, **40**, 1529; (c) S. Couck, J. F. M. Denayer, G. V. Baron, T. Remy, J. Gascon, F. Kapteijn, *J. Am. Chem. Soc.*, 2009, **131**, 6326; (d) O. R. Evans, W. B. Lin, *Acc. Chem. Res.*, 2002, **35**, 511; (e) N. L. Rosi, J. Eckert, M. Eddaoudi, D. T. Vodak, J. Kim, M. Okeeffe, O. M. Yaghi, *Science*, 2003, **300**, 1127; (f) O. M. Yaghi, M. Okeeffe, N. W. Ockwing, H. K. Chae, M. Eddaoudi, J. Kim, *Nature*, 2003, **423**, 705; (g) J. L. C. Rowsell, A. R. Millward, K. S. Park, O. M. Yaghi, *J. Am. Chem. Soc.*, 2004, **126**, 5666; (h) E. Chelebaeva, J. Larionova, Y. Guari, R.A.S. Ferreira, L.D. Carlos, F.A.A. Paz, A. Trifonov, C. Guérin, *Inorg. Chem.* 2009, **48**, 5983; (i) Y.-D. Chiang, M. Hu, Y. Kamachi, S. Ishihara, K. Takai, Y. Tsujimoto, K. Ariga, K.C.-W. Wu, Y. Yamauchi, *Eur. J. Inorg. Chem.* 2013, 3141.
- 2 (a) J.M. Zheng, S.R. Batten, M. Du, *Inorg. Chem.*, 2005, **44**, 3371; (b) P.V. Bernhardt, F. Bozoglian, B.P. Macpherson, M. Martinez, *Coord. Chem. Rev.*, 2005, **249**, 1902. (c) T. Korzeniak, K. Stadnicka, R. Pelka, M. Balanda, K. Tomala, K. Kowalski, B. Sieklucka, *Chem. Commun.*, 2005, 2939; (d) L. Yi, B. Ding, B. Zhao, P. Cheng, D.Z. Liao, S.P. Yan, Z.H. Jiang, *Inorg. Chem.*, 2004, **43**, 33.
- 3 (a) H. Zhang, J. W. Cai, X. L. Feng, B. H. Ye, X. Y. Li, L. N. Ji, *J. Chem. Soc. Dalton Trans.*, 2000, 1687; (b) D. R. Turner, A. S. R. Chesman, K. S. Murray, G. B. Deacon, S. R. Batten, *Chem. Commun.*, 2011, 47, 10189.
- 4 A. H. Yuan, R. Q. Lu, H. Zhou, Y. Y. Chen, Y. Z. Li, *Cryst. Eng. Comm.*, 2010, **12**, 1382.
- 5 C. C. Zhao, W. W. Ni, J. Tao, A. L. Cui, H. Z. Kou, *Cryst. Eng. Comm.*, 2009, **11**, 632.
- 6 K. W. Chapman, P. J. Chupas, C. J. Kepert, *J. Am. Chem. Soc.*, 2005, **127**, 15630.
- 7 Z. Y. Li, N. Wang, J. W. Dai, S. T. Yue, Y. L. Liu, *Cryst. Eng. Comm.*, 2009, **11**, 2003.
- 8 A. L. Goodwin, B. J. Kennedy, C. J. Kepert, *J. Am. Chem. Soc.*, 2009, **131**, 6334.
- 9 A. L. Goodwin, M. Calleja, M. J. Conterio, M. T. Dove, J. S. O. Evans, D. A. Keen, L. Peters, M. G. Tucker, *Science*, 2008, **319**, 794.
- 10 D. P. Zhang, H. L. Wang, L. J. Tian, J. Z. Jiang, Z. H. Ni, *Cryst. Eng. Comm.*, 2009, **11**, 2447.
- 11 G. Beobide, O. Castillo, J. Cepeda, A. Luque, S. Pérez-Yáñez, P. Romána, *Dalton Trans.*, 2009, 9722.
- 12 (a) F. B. Stocker, *Inorg. Chem.*, 1991, **30**, 1472; (b) F. B. Stocker, T. P. Staeva, C. M. Rienstra, D. Britton, *Inorg. Chem.*, 1999, **38**, 984; (c) D. J. Chesnut, D. Plewak, J. Zubietta, *J. Chem. Soc., Dalton Trans.*, 2001, 2567; (d) S. J. Hibble, A. M. Chippindale, *Z. Anorg. Allg. Chem.*, 2005, **631**, 542; (e) T. A. Tronic, K. E. deKrafft, M. J. Lim, A. N. Ley, R. D. Pike, *Inorg. Chem.*, 2007, **46**, 8897; (f) X. He, C.-Z. Lu, D.-Q. Yuan, S.-M. Chen, J.-T. Chen, *Eur. J. Inorg. Chem.*, 2005, **2005**, 2181; (g) K.-M. Park, S. Lee, Y. Kang, S.-H. Moon, S. S. Lee, *Dalton Trans.*, 2008, 6521; (h) S.-Z. Zhan, R. Peng, S.-H. Lin, S. W. Ng, D. Li, *Cryst. Eng. Comm.*, 2010, **12**, 1385; (i) Z. Su, Z. Zhao, B. Zhou, Q. Cai, Y. Zhang, *Cryst. Eng. Comm.*, 2011, **13**, 1474; (j) S. E. H. Etaiw, S. A. Amer, M. M. El-bendary, *Polyhedron*, 2009, **28**, 2385; (k) H. Deng, Y. Qiu, C. Daigebonne, N. Kerbellec, O. Guillou, M. Zeller, S. R. Batten, *Inorg. Chem.*, 2008, **47**, 5866.
- 13 (a) A. Pichon, A. L. Garay, S. L. James, *Cryst. Eng. Comm.*, 2006, **8**, 211; (b) S. Diring, S. Furukawa, Y. Takashima, T. Tsuruoka, S. Kitagawa, *Chem. Mater.*, 2010, **22**, 4531; (c) J. S. Hu, Y. G. Guo, H. P. Liang, L. J. Wang, L. Jiang, *J. Am. Chem. Soc.*, 2005, **127**, 17090; (d) Y. Fan, R. Liu, W. Du, Q. Lu, H. Pangab, F. Gao, *J. Mater. Chem.*, 2012, **22**, 12609.
- 14 (a) M. Basu, A. K. Sinha, M. Pradhan, S. Sarkar, A. Pal, T. Pal, *Chem. Commun.*, 2010, **46**, 8785; (b) X. J. Zhang, G. F. Wang, X. W. Liu, J. J. Wu, M. Li, J. Gu, H. Liu, B. Fang, *J. Phys. Chem. C*, 2008, **112**, 16845; (c) B. Liu, H. C. Zeng, *J. Am. Chem. Soc.*, 2004, **126**, 8124; (d) Z. Y. Zhong, V. Ng, J. Z. Luo, S. P. Teh, J. Teo, A. Gedanken, *Langmuir*, 2007, **23**, 5971.
- 15 (a) W. X. Zhang, M. Li, Q. Wang, G. D. Chen, M. Kong, Z. H. Yang, S. Mann, *Adv. Funct. Mater.*, 2011, **21**, 3516; (b) Z. Y. Wang, F. B. Su, S. Madhavi, X. W. Lou, *Nanoscale*, 2011, **3**, 1618; (c) F. Wang, W. Z. Tao, M. S. Zhao, M. W. Xu, S. C. Yang, Z. B. Sun, L. Q. Wang, X. P. Song, *J. Alloys Compd.*, 2011, **509**, 9798; (d) B. J. C. Park, J. Kim, H. Kwon, H. Song, *Adv. Mater.*, 2009, **21**, 803; (e) S. Y. Gao, S. X. Yang, J. Shu, S. X. Zhang, Z. D. Li, K. Jiang, *J. Phys. Chem. C*, 2008, **112**, 19324.
- 16 B. S. Furniss, A. J. Hannaford, V. Rogers, P. W. G. Smith, A. R. Tatchell, *Vogel's Textbook of Practical Organic Chemistry*, 4th Edn., Longman, London, 1978.
- 17 G. M. Sheldrick, *Acta Crystallogr., Sect. A: Found. Crystallogr.*, 2007, **64**, 112.
- 18 (a) G. M. Sheldrick, SHELX-97; Programme for Refinement of Crystal Structures, University of Gottingen, Gottingen, Germany, 1997; (b) A. L. Spek, PLATON, *Acta Cryst.*, 1990, **46A**, C34.
- 19 (a) C. A. Bayse, T. P. Brewster, R. D. Pike, *Inorg. Chem.*, 2009, **48**, 174; (b) B. Liu, L. Xu, G.-C. Guo, J.-S. Huang, *Inorg. Chem. Commun.*, 2005, **8**, 796.
- 20 (a) S. Jammie, S. Sakthivel, L. Rout, T. Mukherjee, S. Mandal, R. Mitra, P. Saha, T. Punniyamurthy, *J. Org. Chem.*, 2009, **74**, 1971; (b) L. Rout, S. Jammie, T. Punniyamurthy, *Org. Lett.*, 2007, **9**, 3397; (c) L. Rout, T. K. Sen, T. Punniyamurthy, *Angew. Chem. Int. Ed.*, 2007, **46**, 5583.